



ELSEVIER

Comput. Methods Appl. Mech. Engrg. 191 (2002) 2297–2315

**Computer methods
in applied
mechanics and
engineering**

www.elsevier.com/locate/cma

Analysis of thin piezoelectric solids by the boundary element method

Yijun Liu*, Hui Fan

Department of Mechanical Engineering, University of Cincinnati, P.O. Box 210072, Cincinnati, OH 45221-0072, USA

Received 21 February 2001; received in revised form 1 October 2001

Abstract

The piezoelectric boundary integral equation (BIE) formulation is applied to analyze thin piezoelectric solids, such as thin piezoelectric films and coatings, using the boundary element method (BEM). The nearly singular integrals existing in the piezoelectric BIE as applied to thin piezoelectric solids are addressed for the 2-D case. An efficient analytical method to deal with the nearly singular integrals in the piezoelectric BIE is developed to accurately compute these integrals in the piezoelectric BEM, no matter how close the source point is to the element of integration. Promising BEM results with only a small number of elements are obtained for thin films and coatings with the thickness-to-length ratio as small as 10^{-6} , which is sufficient for modeling many thin piezoelectric films as used in smart materials and micro-electro-mechanical systems. © 2002 Elsevier Science B.V. All rights reserved.

Keywords: Piezoelectric films; Boundary integral equation; Nearly singular integrals; Boundary element method

1. Introduction

In recent years, piezoelectric materials have been used widely as sensors and actuators in smart materials and micro-electro-mechanical systems (MEMS), because piezoelectric materials possess many desirable properties [1–3]. Analysis of the piezoelectric sensors and actuators is, however, very difficult because they are usually made in the forms of thin films or coatings applied on elastic substrates. Detailed stress analysis for durability assessment of such materials is challenging for any numerical methods based on the piezoelectric plate or shell theories, especially in evaluating interface stresses which exhibit singularities near the edges of the films (see e.g., Ref. [4]). To ensure the highest possible accuracy in the stress or fracture analysis of the delicate piezoelectric films and coatings, accurate 2-D or 3-D models based on the piezoelectricity theory should be employed.

* Corresponding author. Tel.: +1-513-556-2738; fax: +1-513-556-3390.
E-mail address: yijun.liu@uc.edu (Y.J. Liu).

In the last decade, there have been increasing efforts in the research on modeling piezoelectric materials using the boundary integral equation/boundary element method (BIE/BEM) based on the 2-D or 3-D piezoelectricity theory. For example, Lee and Jiang [5–7] developed the BEM formulation for piezoelectric solids and tested their method on a 2-D infinite piezoelectric medium with a cylindrical hole [7]. A 3-D BEM for piezoelectric solids was developed by Chen and Lin [8], based on the fundamental solutions derived earlier [9,10] for 3-D piezoelectric solids. The numerical examples using linear elements on a piezoelectric cube and a spherical cavity were presented in [8]. Hills and Farris [11] applied the quadratic (eight node) boundary elements for 3-D piezoelectric bodies and tested their approach on the cube and spherical void problems. Ding et al. [12,13] derived the fundamental solutions in terms of harmonic functions and developed the BEM with several test cases for 2-D [12] and 3-D problems [13]. Recently, Jiang [14] derived the fundamental solutions and the BIE for 3-D time-dependent thermo-piezoelectricity. For piezoelectric solids with defects (various voids and cracks), Xu and Rajapakse [15] studied the influence and interactions of various holes in 2-D piezoelectric media using a coupled BEM. Zhao et al. [16,17] derived the 3-D fundamental solutions and the BIE for a penny-shaped crack in a piezoelectric solid. Pan [18] recently presented a detailed study on cracks in 2-D piezoelectric media using the BEM. Both the conventional BIE and a hypersingular BIE (traction BIE) were employed in [18] to handle the degeneracy of the BIEs for crack problems. Recently, Qin [19] studied the cracks in a piezoelectric half plane under thermal loading with the BEM.

All the above results using the BEM have clearly demonstrated the accuracy and efficiency of the piezoelectric BEM, especially in stress and fracture analyses, for single and *bulky* piezoelectric materials. However, no piezoelectric BEM has been attempted to analyze *thin* piezoelectric materials, such as piezoelectric films and coatings. Applications of the piezoelectric BEM to thin piezoelectric structures face two crucial questions: (1) Does the piezoelectric BIE degenerate when applied to shell-like piezoelectric structures? (2) How to deal with the nearly singular integrals existing in the piezoelectric BIE when applied to shell-like and crack-like problems? The first question has been addressed in a recent paper [20] which proves that the piezoelectric BIE does *not* degenerate when applied to thin piezoelectric shell-like structures, contrary to the case of modeling cracks in piezoelectric materials using the BIE. Related discussions on this issue in the context of thin *elastic* structures using the BEM can be found in Refs. [21,22]. However, according to the best knowledge of the authors, no work has been reported in the literature to address the second question regarding the nearly singular integrals in the piezoelectric BIE when applied to shell-like piezoelectric structures.

In the context of elastic structures or materials, it has been demonstrated that the BIE/BEM with thin-body capabilities can handle various thin shell-like problems very effectively, regardless of the thinness of the structures, or non-uniform thickness, as long as the nearly singular integrals are computed accurately. Numerous examples of applying the BEM based on the elasticity theory to both 2-D and 3-D thin shell-like structures, including thin elastic layered films, coatings, interphases in composites, with or without interface cracks, can be found in Refs. [21,23–29]. These studies have shown that accurate, efficient, and yet stable displacement and stress results can be obtained using the BEM for the analysis of the thin structures or materials with the thickness-to-length ratios in the range of 10^{-6} – 10^{-9} , once the nearly singular integrals are computed accurately. The semi-analytical approach for 3-D case and the analytical approach for 2-D case developed in the above mentioned work to deal with the nearly singular integrals in the elasticity BIEs can be extended to the 2-D piezoelectric BIE with no new conceptual challenges, although it is much more involved for the piezoelectric BIE case.

In this paper, a piezoelectric BEM is developed for analyzing 2-D thin piezoelectric structures with very small thickness-to-length ratios. The nearly singular integrals (line integrals for 2-D problems) are transformed into integrals containing summations of several polynomial fractions, which can be computed analytically. For the test problems on piezoelectric films, coatings and beams, very promising BEM results with only a few boundary elements are obtained when the thickness-to-length ratio is as small as 10^{-6} . This

is sufficient for modeling most thin piezoelectric materials in various applications such as smart materials and MEMS.

2. The boundary integral equation formulation for piezoelectricity

Consider a piezoelectric solid occupying a domain V with the boundary S (Fig. 1). The basic equations governing the elastic and electric fields in a linear piezoelectric material can be summarized in the following (see e.g., Refs. [1,6,8,20]) (index notation is used here).

Equilibrium equations:

$$\sigma_{ij,j} + f_i = 0, \tag{1}$$

$$D_{i,i} - q = 0, \tag{2}$$

where σ_{ij} is the stress tensor, f_i is the body force vector per unit volume, D_i is the electric displacement vector and q is the intrinsic electric charge per unit volume.

Constitutive equations:

$$\sigma_{ij} = C_{ijkl}s_{kl} - e_{kij}E_k \text{ (converse effect),} \tag{3}$$

$$D_i = e_{ikl}s_{kl} + \varepsilon_{ik}E_k \text{ (direct effect),} \tag{4}$$

where s_{kl} is the strain tensor, E_k is the electric field, C_{ijkl} is the elastic modulus tensor measured in a constant electric field, e_{ijk} is the piezoelectric tensor and ε_{ij} is the dielectric tensor measured at constant strains.

Strain and electric fields:

$$s_{ij} = \frac{1}{2}(u_{i,j} + u_{j,i}), \tag{5}$$

$$E_i = -\phi_{,i}, \tag{6}$$

where u_i is the elastic displacement vector and ϕ is the electric potential.

Boundary conditions (BCs):

$$t_i = \sigma_{ij}n_j = \bar{t}_i, \quad \text{on } S_t, \quad u_i = \bar{u}_i, \quad \text{on } S_u \text{ (mechanical BCs),} \tag{7}$$

$$\omega = -D_i n_i = \bar{\omega}, \quad \text{on } S_\omega, \quad \phi = \bar{\phi}, \quad \text{on } S_\phi \text{ (electric BCs),} \tag{8}$$

where t_i is the traction, ω is the surface charge, n_i is the unit outward normal vector (Fig. 1) and the barred quantities indicate given values. Note that the boundary $S = S_t \cup S_u = S_\omega \cup S_\phi$.

Eqs. (1)–(6) under BC (7), (8) form the complete mathematical description of the coupled elastic and electric fields in a general anisotropic piezoelectric solid. The above differential governing equations can be

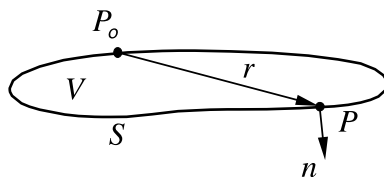


Fig. 1. A thin piezoelectric solid V with boundary S .

formulated in BIEs using the reciprocal theorem and the fundamental solutions for the piezoelectric solid (see e.g., Ref. [20]). For 2-D problems in analyzing piezoelectric materials, the representation integral is given as follows (matrix notation is used here; see Refs. [12,20]):

$$\mathbf{u}(P_0) = \int_S \mathbf{U}(P, P_0) \mathbf{t}(P) dS(P) - \int_S \mathbf{T}(P, P_0) \mathbf{u}(P) dS(P) + \int_V \mathbf{U}(P, P_0) \mathbf{b}(P) dV(P), \quad \forall P_0 \in V, \quad (9)$$

in which

$$\mathbf{u} = \begin{Bmatrix} u_1 \\ u_2 \\ -\phi \end{Bmatrix}, \quad \mathbf{t} = \begin{Bmatrix} t_1 \\ t_2 \\ -\omega \end{Bmatrix}, \quad \mathbf{b} = \begin{Bmatrix} f_1 \\ f_2 \\ -q \end{Bmatrix}, \quad \mathbf{U} = \begin{bmatrix} U_{11} & U_{12} & U_{13} \\ U_{21} & U_{22} & U_{23} \\ U_{31} & U_{32} & U_{33} \end{bmatrix}, \quad \mathbf{T} = \begin{bmatrix} T_{11} & T_{12} & T_{13} \\ T_{21} & T_{22} & T_{23} \\ T_{31} & T_{32} & T_{33} \end{bmatrix} \quad (10)$$

are the generalized (or extended) displacement, traction and body force vectors, and the generalized displacement and traction kernels in the 2-D piezoelectric fundamental solutions (see Appendix), respectively; P_0 the source point and P the field point. Note that the dimensions of matrices are 3×3 for 2-D piezoelectric problems because of the coupling of the elastic and electric fields.

Let the source point P_0 go to the boundary S in the above representation integral, we obtain the piezoelectric boundary integral equation in the traditional (singular) form:

$$\mathbf{C}(P_0) \mathbf{u}(P_0) + \int_S \mathbf{T}(P, P_0) \mathbf{u}(P) dS(P) = \int_S \mathbf{U}(P, P_0) \mathbf{t}(P) dS(P) + \int_V \mathbf{U}(P, P_0) \mathbf{b}(P) dV(P), \quad \forall P_0 \in S, \quad (11)$$

where \mathbf{C} is a 3×3 coefficient matrix depending on the smoothness of S at P_0 .

Applying the integral identity for the piezoelectric fundamental solution developed in Ref. [20], we can obtain the following *weakly singular form* of the boundary integral equation for piezoelectricity [20]:

$$\int_S \mathbf{T}(P, P_0) [\mathbf{u}(P) - \mathbf{u}(P_0)] dS(P) = \int_S \mathbf{U}(P, P_0) \mathbf{t}(P) dS(P) + \int_V \mathbf{U}(P, P_0) \mathbf{b}(P) dV(P), \quad \forall P_0 \in S, \quad (12)$$

for a *finite* piezoelectric solid (cf., the potential and elasticity cases [30–33]).

The weakly singular BIE (12) for piezoelectric solids has several advantages, compared with the singular BIE (11). There are no singular integrals in the weakly singular BIE and its discretization leads directly to the conclusion that the diagonal terms can be determined by summing the off-diagonal terms for the matrix involving the singular kernel \mathbf{T} (see Ref. [30]). By employing weakly singular BIE (12), one does not need to evaluate any jump terms explicitly in deriving the piezoelectric BIEs. In recent years, regularizing the singular integrals in the BIEs has become a common approach to dealing with the singular integrals in the BEM [34,35].

As discussed in Section 1, before the piezoelectric BIE (12) can be applied to analyze thin piezoelectric structures, an accurate and efficient method needs to be developed to deal with the nearly singular integrals existing in BIE (12) for such problems. Section 3 is a first attempt to address this crucial issue.

3. Nearly singular integrals in the piezoelectric BIE for thin shapes

The numerical difficulty in applying the piezoelectric BEM based on BIE (12) is the treatment of the nearly singular integrals which arise in both crack-like and thin shell-like problems. The integrals in the

BIE, which determine the influence matrices, contain singular kernels of order $O(1/r)$ and $O(\ln r)$ in 2-D piezoelectricity case (same as in the elasticity case), where r is the distance between the source point P_0 and the field (integration) point P (Fig. 1). When the source point is very close to, but not on an element of integration, although the kernels are regular in the mathematical sense, values of the kernels can change rapidly on that element [23]. The standard Gaussian quadrature is no longer accurate or efficient in this case since a large number of integration points or many subdivisions of the element are needed in order to achieve the required accuracy [36]. Even the weakly singular form of the BIE, such as BIE (12), can not avoid this nearly singular integral difficulty. As discussed in Refs. [21,23,36,37] for the 2-D and 3-D elasticity BIE cases, a very accurate and yet efficient approach to deal with these nearly singular integrals is to evaluate them analytically through some manipulations. Although the case for the piezoelectric BIE is much more complicated due to the lengthy expressions for the piezoelectric fundamental solution [5–7], it is still possible to evaluate the nearly singular integrals analytically as in the elasticity BIE case.

We first consider the integral in BIE (11) or (12) containing the singular kernel T_{ij} when the source point is close to but not on the element of integration. By subtracting and adding back a term in the following manner, the nearly singular integral can be rewritten as (see Refs. [21,23,36] for details):

$$\int_{\Delta L} T_{ij}(P, P_0)u_j(P) dL(P) = \int_{\Delta L} T_{ij}(P, P_0)[u_j(P) - u_j(P'_0)] dL(P) + u_j(P'_0) \int_{\Delta L} T_{ij}(P, P_0) dL(P), \quad (13)$$

where ΔL is the line element under consideration, P'_0 is the closest point on the element to P_0 (an image point of P_0 on the element [21,23,36]). Note that the indices i and j run from 1 to 3 for the 2-D piezoelectric BIE case (see Eq. (10)). As $P \rightarrow P'_0$, the term $u_j(P) - u_j(P'_0)$ has the order of $O(r')$, with r' being the distance from P'_0 to P . The order of the first integral on the right-hand side of (13) is reduced to $O(r')/O(r)$. This integral is a nearly weakly singular integral, which can be evaluated accurately by a non-linear coordinate transformation developed for the 2-D elasticity case in Ref. [23]. Now we focus on the evaluation of the last integral in (13) containing only the singular kernel T_{ij} by using an analytical approach.

Let us analyze the expressions of the T_{ij} kernel first. For 2-D piezoelectric problems, the fundamental solution is much more complicated and the expressions for the corresponding kernels are very lengthy, as first presented in Refs. [5–7]. For brevity and clarity, we only list the major expressions here and leave the other expressions in the Appendix and the references therein. The T_{ij} kernel for the 2-D piezoelectric fundamental solution can be expressed as (see Appendix):

$$\begin{aligned} T_{11} &= (c_{11}U_{111} + c_{12}U_{122} + e_{21}U_{132})n_1 + (c_{33}(U_{112} + U_{121}) + e_{13}U_{131})n_2, \\ T_{21} &= (c_{11}U_{211} + c_{12}U_{222} + e_{21}U_{232})n_1 + (c_{33}(U_{212} + U_{221}) + e_{13}U_{231})n_2, \\ T_{31} &= (c_{11}U_{311} + c_{12}U_{322} + e_{21}U_{332})n_1 + (c_{33}(U_{312} + U_{321}) + e_{13}U_{331})n_2, \\ T_{12} &= (c_{12}U_{111} + c_{22}U_{122} + e_{22}U_{132})n_2 + (c_{33}(U_{112} + U_{121}) + e_{13}U_{131})n_1, \\ T_{22} &= (c_{12}U_{211} + c_{22}U_{222} + e_{22}U_{232})n_2 + (c_{33}(U_{212} + U_{221}) + e_{13}U_{231})n_1, \\ T_{32} &= (c_{12}U_{311} + c_{22}U_{322} + e_{22}U_{332})n_2 + (c_{33}(U_{312} + U_{321}) + e_{13}U_{331})n_1, \\ T_{13} &= -(e_{13}(U_{112} + U_{121}) - \varepsilon_{11}U_{131})n_1 - (e_{21}U_{111} + e_{22}U_{122} - e_{22}U_{132})n_2, \\ T_{23} &= -(e_{13}(U_{212} + U_{221}) - \varepsilon_{11}U_{231})n_1 - (e_{21}U_{211} + e_{22}U_{222} - e_{22}U_{232})n_2, \\ T_{33} &= -(e_{13}(U_{312} + U_{321}) - \varepsilon_{11}U_{331})n_1 - (e_{21}U_{311} + e_{22}U_{322} - e_{22}U_{332})n_2, \end{aligned} \quad (14)$$

where n_1 and n_2 are directional cosines of the normal n ; $c_{11}, \dots, e_{11}, \dots$, and ε_{11}, \dots are the elastic modulus, piezoelectric and dielectric constants, respectively (in the matrix notation); and U_{ijk} are the spatial derivatives of the U_{ij} kernel (see Appendix).

From the lengthy expressions (A.4)–(A.6) listed in the Appendix, we can conclude that the T_{ij} kernel can be written in the following form:

$$T_{ij} = \sum_{m=1}^{12} (C_{m1}X_m n_1 + C_{m2}X_m n_2), \tag{15}$$

where C_{mk} are combinations of the constants, and X_m is one of the g_{ij} terms defined in (A.4) in the Appendix. Thus we can write:

$$\begin{aligned} \int_{\Delta L} T_{ij}(P, P_0) dL(P) &= \int_{\Delta L} \sum_{m=1}^{12} (C_{m1}X_m n_1 + C_{m2}X_m n_2) dL(P) \\ &= \sum_{m=1}^{12} \left[C_{m1} \int_{\Delta L} X_m n_1 dL(P) + C_{m2} \int_{\Delta L} X_m n_2 dL(P) \right]. \end{aligned} \tag{16}$$

That is, the integration of T_{ij} can be determined by the integrations of $X_m n_1$ and $X_m n_2$ on the element ΔL .

Apply quadratic line elements on the boundary and assume that the coordinates of the three nodes of the element of integration are (x_1, y_1) , (x_2, y_2) (middle node) and (x_3, y_3) , and the source point is (x_0, y_0) . Employing the quadratic shape functions:

$$N_1(\xi) = (\xi - 1)\xi/2, \quad N_2(\xi) = 1 - \xi^2, \quad N_3(\xi) = (\xi + 1)\xi/2,$$

with ξ ($-1 \leq \xi \leq 1$) being the natural coordinate, we have

$$\begin{aligned} r_1 = x - x_0 &= \sum_{\alpha=1}^3 N_{\alpha} x_{\alpha} - x_0 = \frac{x_1 + x_3 - 2x_2}{2} \xi^2 + \frac{x_3 - x_1}{2} \xi + x_2 - x_0, \\ r_2 = y - y_0 &= \sum_{\alpha=1}^3 N_{\alpha} y_{\alpha} - y_0 = \frac{y_1 + y_3 - 2y_2}{2} \xi^2 + \frac{y_3 - y_1}{2} \xi + y_2 - y_0. \end{aligned} \tag{17}$$

That is, r_1 and r_2 are quadratic functions of ξ . On the element, it can be shown that

$$\begin{aligned} n_1 &= \frac{1}{J} \left[(y_1 + y_3 - 2y_2)\xi + \frac{y_3 - y_1}{2} \right], \\ n_2 &= -\frac{1}{J} \left[(x_1 + x_3 - 2x_2)\xi + \frac{x_3 - x_1}{2} \right], \\ dL &= J d\xi, \end{aligned} \tag{18}$$

where J is the Jacobian. Therefore, for a typical integral in (16) we obtain

$$\int_{\Delta L} X_m n_1 dL(P) = \int_{-1}^1 X_m \left[(y_1 + y_3 - 2y_2)\xi + \frac{y_3 - y_1}{2} \right] d\xi. \tag{19}$$

Substituting the expressions (17) for r_1 and r_2 into X_m , which in turn is one of the terms in (A.4) in the Appendix, the above formula (19) can be shown to have the following final form:

$$\int_{\Delta L} X_m n_1 dL(P) = \int_{-1}^1 \frac{a\xi^3 + b\xi^2 + c\xi + d}{e\xi^4 + f\xi^3 + g\xi^2 + h\xi + q} d\xi, \tag{20}$$

where constants $a-q$ are combinations of the nodal coordinates and the material constants. Note that the constants e, f, g, h and q in (20) cannot be zero at the same time. It is also found from the numerical tests that the denominator of the integrand in (20) has no roots in the interval $[-1, 1]$. The integration of $X_m n_2$ is handled in a similar way.

In general, an integral like (20) can be integrated analytically, given constants $a-q$ (for example, using a symbolic manipulation software). Then integrals in (16) can be determined easily. In this way, we can convert the last integral in (13) containing the singular kernel to the summation of integrals containing polynomial fractions like (20), and these polynomial fraction integrals (20) do not depend on the integration path ΔL . There is no difficulty at all in obtaining the exact values of such integrals, no matter how close the source point is to the element.

For the nearly weakly singular integrals, that is, the one containing the U_{ij} kernel in BIE (12) and the first integral on the right-hand side of (13), the non-linear coordinate transformation developed in [23] for 2-D elasticity BIE is applied in the current study. It is found that this technique is equally effective and efficient in the case of the 2-D piezoelectric BIE.

4. Numerical examples

To verify the procedures presented in the previous section for dealing with the nearly singular integrals in the piezoelectric BIE, a 2-D piezoelectric BEM program is developed and three numerical test problems are studied in which the BEM solutions are obtained and compared with the analytical solutions when they are available.

4.1. Test problem 1: a thin piezoelectric film

First, a thin piezoelectric film under a uniform stretch \bar{u} in the x direction (Fig. 2) is studied, for which analytical solution can be found readily. We assume the dimension of the film in the z direction is very large so that it can be considered as a plane strain problem. The length L of the film is constant ($= 1$ m here), while the thickness h changes from L to $10^{-6} L$. Note that the thickness h is changing from the macro- to micro-scales, relative to the length L , which may already be outside of the limits of the continuum mechanics assumptions for many materials. However, it is of more interest here to verify the validity and effectiveness of developed advanced BEM approach for such 2-D thin piezoelectric materials.

The boundary of the film is discretized with 10 quadratic boundary elements, with four elements on each of the two horizontal (long) edges and one element on each of the two vertical (short) edges. For the *mechanical BC*, displacement in the y direction is constrained along the edge $y = 0$; displacement in the x

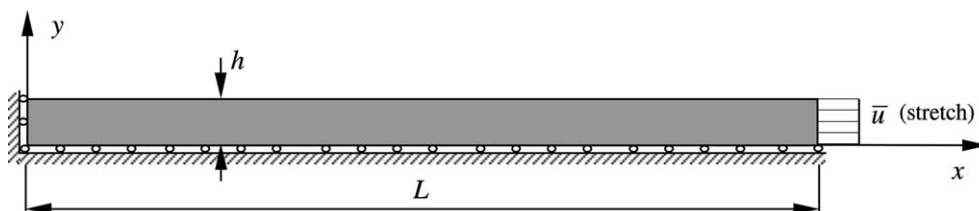


Fig. 2. A thin piezoelectric film.

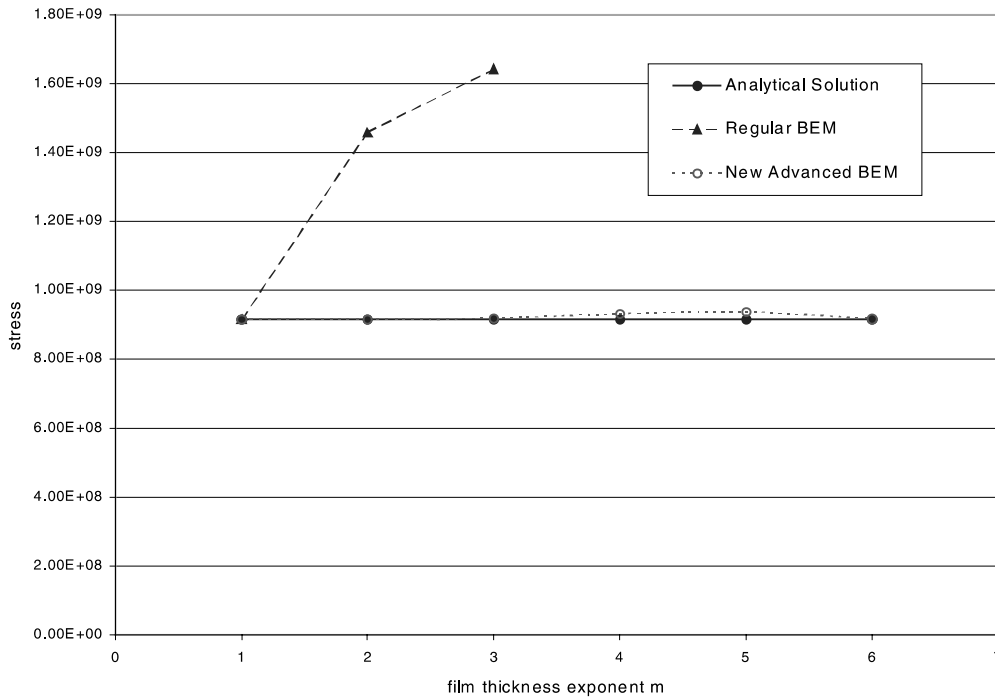


Fig. 3. Stress σ_x at point (L, h) with the piezoelectric BEMs ($h/L = 10^{-m}$).

direction is constrained along the edge $x = 0$; the specified stretch $\bar{u} = 0.01$ m and traction-free conditions are applied on other boundaries and directions (Fig. 2). For the *electric* BC, the electric potential is zero along the top and bottom edges; and the surface charge is zero on the two vertical edges. No body forces and changes are applied to the piezoelectric body. The material used is PZT-4 and the material constants (in the matrix notation) are given below [7]:

$$\text{elastic modulus: } c_{11} = 14.1, \quad c_{22} = 11.6, \quad c_{33} = 2.53, \quad c_{12} = 7.57 \quad (10^{10} \text{ N/m}^2);$$

$$\text{piezoelectric constants: } e_{21} = -5.3, \quad e_{22} = 15.5, \quad e_{13} = 13.0 \quad (\text{C/m}^2);$$

$$\text{dielectric constants: } \varepsilon_{11} = 6.37, \quad \varepsilon_{22} = 5.53 \quad (10^{-9} \text{ C/V m}).$$

Fig. 3 shows the results of stress σ_x at the upper-right corner, for different thicknesses of the film, using the regular piezoelectric BEM (without employing the techniques for dealing with the nearly singular integrals) and the new BEM presented in this paper. It is obvious that the regular BEM results deteriorate quickly as the thickness decreases (“ m ” in the plot represents the exponent in the thickness, e.g., “ $m = 1$ ” means $h = 10^{-1}L$). Data at $m = 4, 5$ and 6 are not plotted for the regular BEM, since they are meaningless due to the poor accuracies of the integration schemes in the regular BEM for such thin piezoelectric solid case. The same conclusion was made in Refs. [21,23] for the 3-D and 2-D thin *elastic* solid cases. For the advanced piezoelectric BEM using the techniques for dealing with the nearly singular integrals, as discussed in Section 3, we notice that for all the thickness-to-length ratios h/L down to 10^{-6} , the results are still very accurate and stable, with the maximum error (at $h/L = 10^{-5}$) less than 3% (the better accuracy at

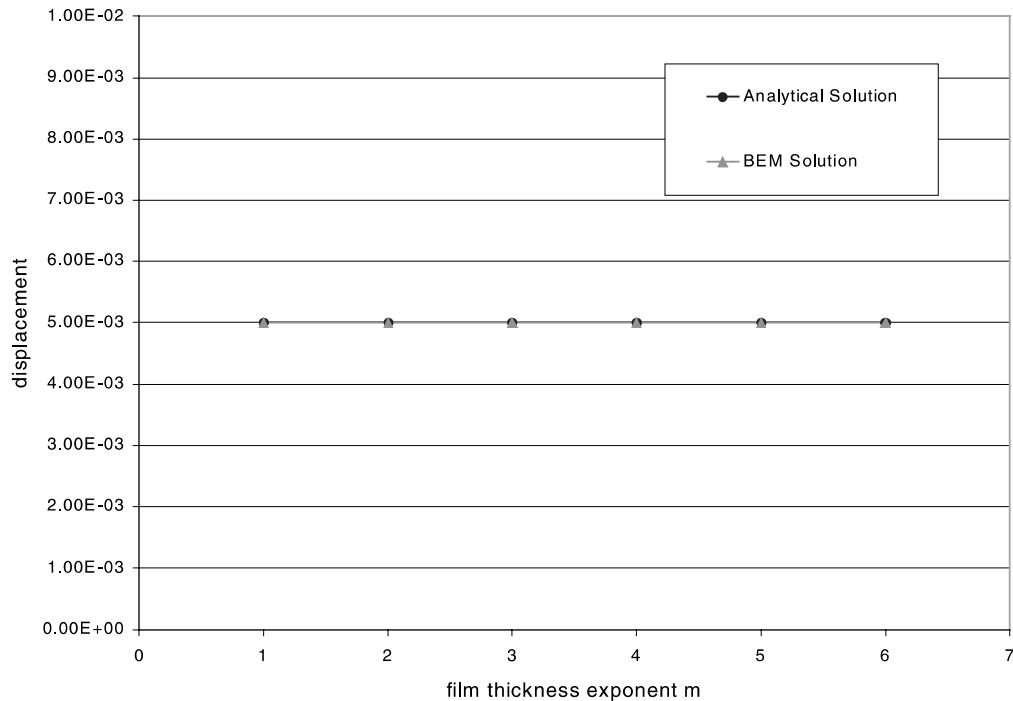


Fig. 4. The x -component of displacement at point $(L/2, 0)$.

$h/L = 10^{-6}$ is purely a coincidence). From hereafter, all the BEM results reported are obtained by using the new advanced BEM presented in the previous sections.

The BEM results for the x -displacement of the point $(L/2, 0)$ (Fig. 4) are very accurate for this example as well, almost reproducing the exact values. The BEM results for the surface charge at the point $(L/2, 0)$ (Fig. 5) are also very close to the values from the analytical solution, with all the errors less than 3%. All these BEM results demonstrate that the developed analytical method for dealing with the nearly singular integrals in the piezoelectric BEM procedure is very effective and accurate. It is also shown that the piezoelectric BIE does not degenerate when applied to thin shell-like piezoelectric structures, as proved analytically in Ref. [20].

4.2. Test problem 2: piezoelectric coating on a rigid cylinder

We next study the case of a rigid cylinder covered with a thin piezoelectric (PZT-4) coating (Fig. 6). The radius of the cylinder a is fixed ($= 1$ m here), while the thickness of the coating h is reduced to test the developed piezoelectric BEM on this case with curved boundaries. For the *mechanical BC*, the coating is subjected to a uniform pressure load p at the outer boundary, and is fixed at the inner boundary (interface with the rigid cylinder). For the *electric BC*, zero surface charge is applied on both inner and outer boundaries. When the thickness h decreases, the radial stress at the interface (e.g., point A , Fig. 6) should approach the value of the applied pressure, while the mechanical displacement at the outer boundary should approach zero. These can be employed to verify the BEM solutions.

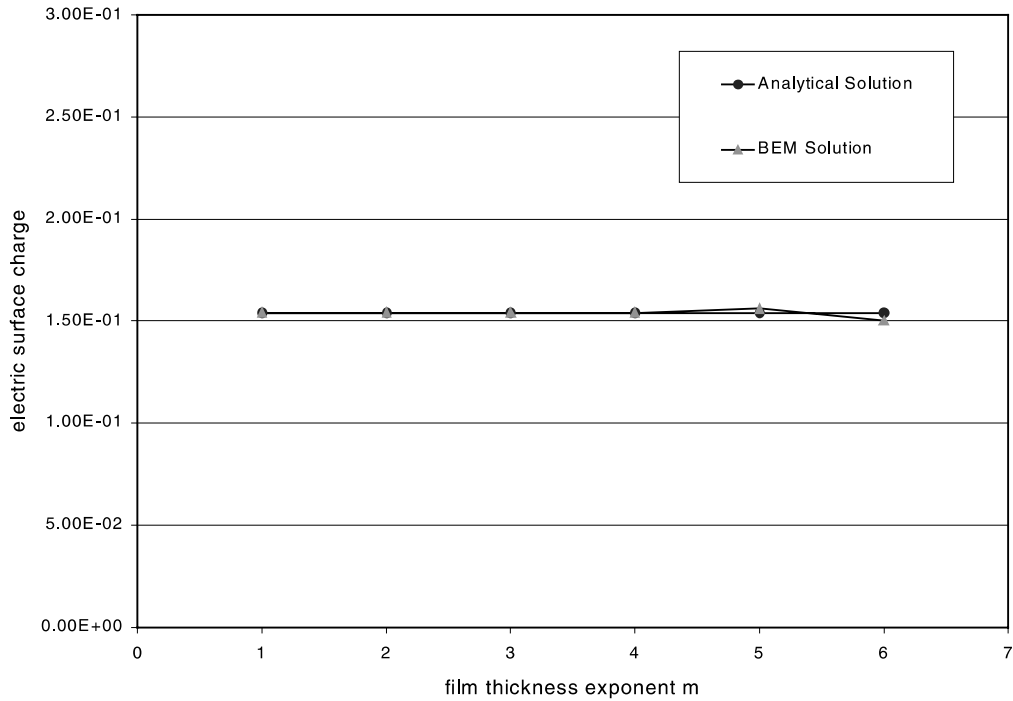


Fig. 5. The electric surface charge at point $(L/2, 0)$.

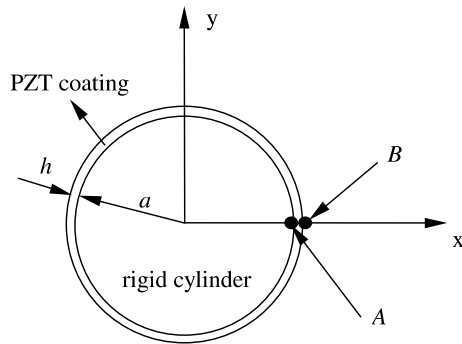


Fig. 6. A rigid cylinder with a thin piezoelectric coating under pressure p .

Two BEM meshes with very small numbers of elements are used for the coating, one with eight quadratic elements (four elements on each circular boundary) and another one with 16 quadratic elements (eight elements on each circle). Fig. 7 shows the results for the radial stress at point A (interface) with the two boundary element discretizations, as the thickness of the PZT-4 coating decreases from $h = 10^{-0.301}a$ ($=0.5a$), $10^{-1}a$, $10^{-2}a$, \dots , to $10^{-5}a$. Both the BEM interface stress results approach the applied pressure p

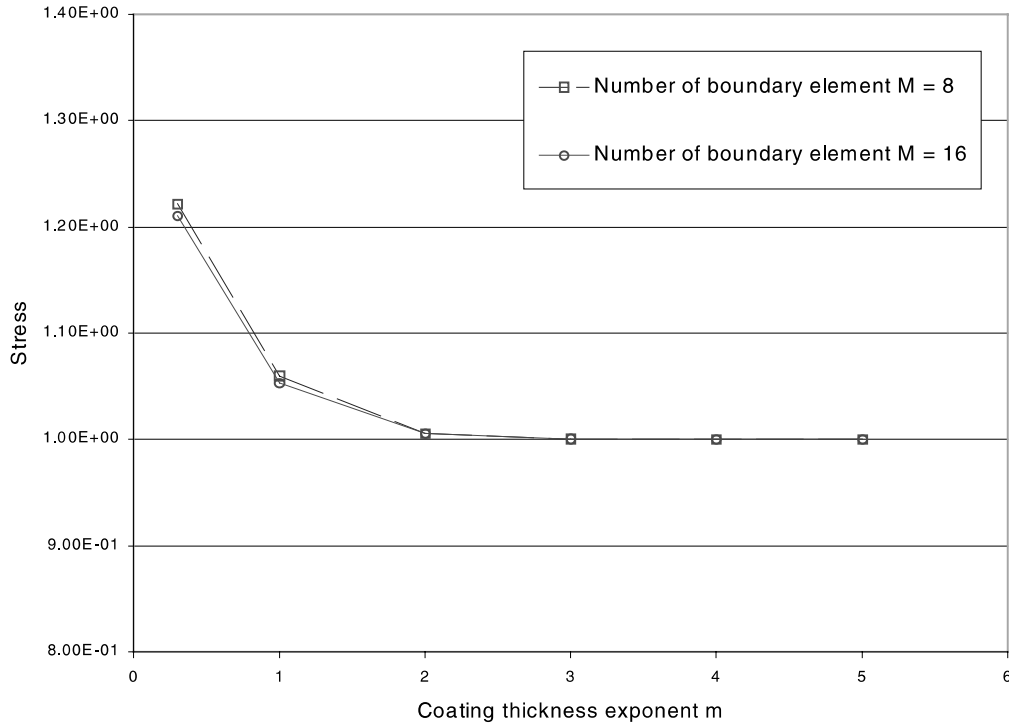


Fig. 7. Magnitude of the stress $\sigma_x (\times p)$ at point $A (h/a = 10^{-m})$.

as the thickness decreases, which is expected. Fig. 8 gives the mechanical displacement (radial component) at point B , while Fig. 9 shows the electric displacement (tangential component) at point B . Both the mechanical and electric displacement components vanish with the decrease of the coating thickness, which is also expected.

This example demonstrates that the developed piezoelectric BEM for thin shell-like structures can handle models of curved boundaries very efficiently and accurately as well. Stable and converged BEM results can be obtained with a small number of boundary elements, regardless how small the thickness of the piezoelectric coating is.

4.3. Test problem 3: a piezoelectric strip under a combined mechanical and electric load

A piezoelectric (PZT-5) strip under a combined loading of pressure p and voltage V_0 (Fig. 10) is studied next. This is the same example problem as presented in Ref. [38]. The polarization direction of the piezoelectric strip is in the z direction. The analytical solution for this problem can be derived readily and is given as Eqs. (87)–(89) in Ref. [38] (where the symbol “ h ” in Eq. (88) should be replaced by “ $L/2$ ”) and is employed here to validate the developed piezoelectric BEM for thin piezoelectric solids under shear deformation. The mechanical boundary conditions are as shown in Fig. 10, while the electrical boundary conditions are:

$$\phi = V_0, \quad \text{at } x = 0; \quad \text{and} \quad \phi = -V_0, \quad \text{at } x = L;$$

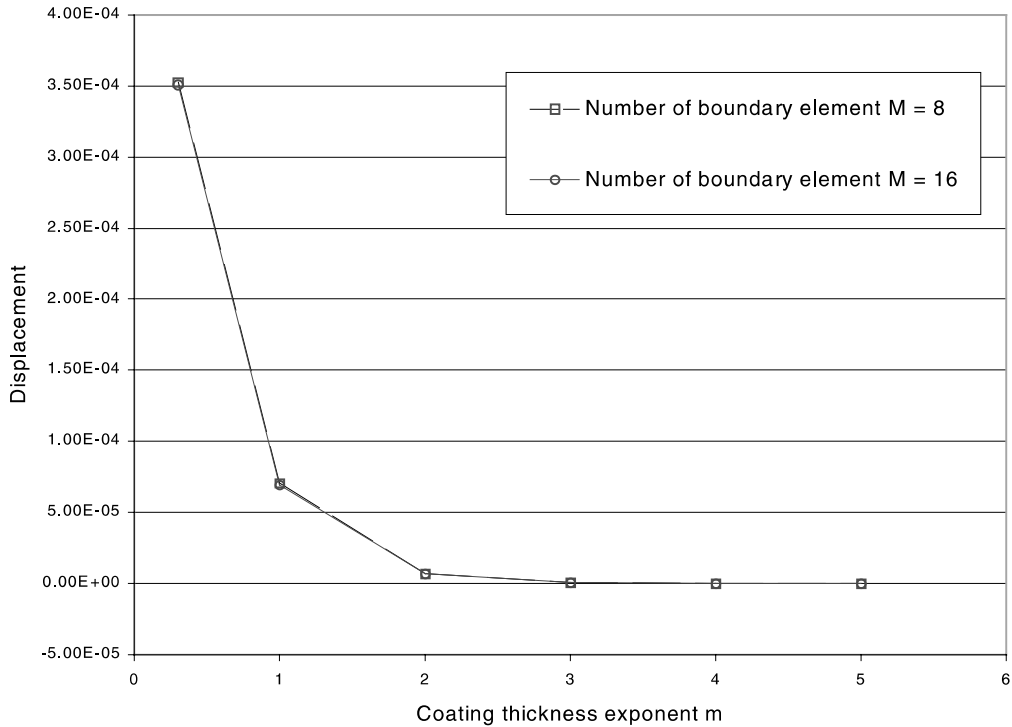


Fig. 8. Magnitude of the mechanical displacement u_x ($\times p$) at point B .

$$\frac{\partial \phi}{\partial z} = 0, \quad \text{at } z = \pm h.$$

The length of the strip used is fixed at $L = 1$ mm, while the thickness $2h$ is changed from L to $10^{-4}L$. The applied pressure $p = 5$ N/mm² and the voltage $V_0 = 1000$ V, as used in Ref. [38]. The shear deformation dominates under these conditions, due to the applied voltages along the two vertical edges [38]. This piezoelectric beam-like model can be viewed as a simple piezoelectric device which converts the applied electric field into deflection of the beam for sensing or actuating purposes. The material constants used for PZT-5 are given below:

elastic modulus: $c_{11} = 7.3383$, $c_{22} = 6.4015$, $c_{33} = 2.1053$, $c_{12} = 2.8182$ (10^4 N/mm²);

piezoelectric constants: $e_{21} = -2.0817$, $e_{22} = 19.0942$, $e_{13} = 12.2947$ (10^{-3} N/(mm V));

dielectric constants: $\epsilon_{11} = 0.8130$, $\epsilon_{22} = 14.3001$ (10^{-8} N/V²).

A total of 16 boundary elements (four on each edge) are used in the analysis using the developed piezoelectric BEM and converged results are obtained. Further increase of the elements does not show any significant changes in the results. Fig. 11 shows the BEM results of the displacement component w along the bottom edge of the PZT-5 strip, as compared with the analytical solutions, for three different values of the thickness $2h$. Again, the BEM results are very accurate (with maximum error less than 2%) for all the thin strip cases. It is also noticed that the shear deformation is insensitive to the thickness of the strip when it is thin. This example demonstrates that the developed BEM can handle the combined loading

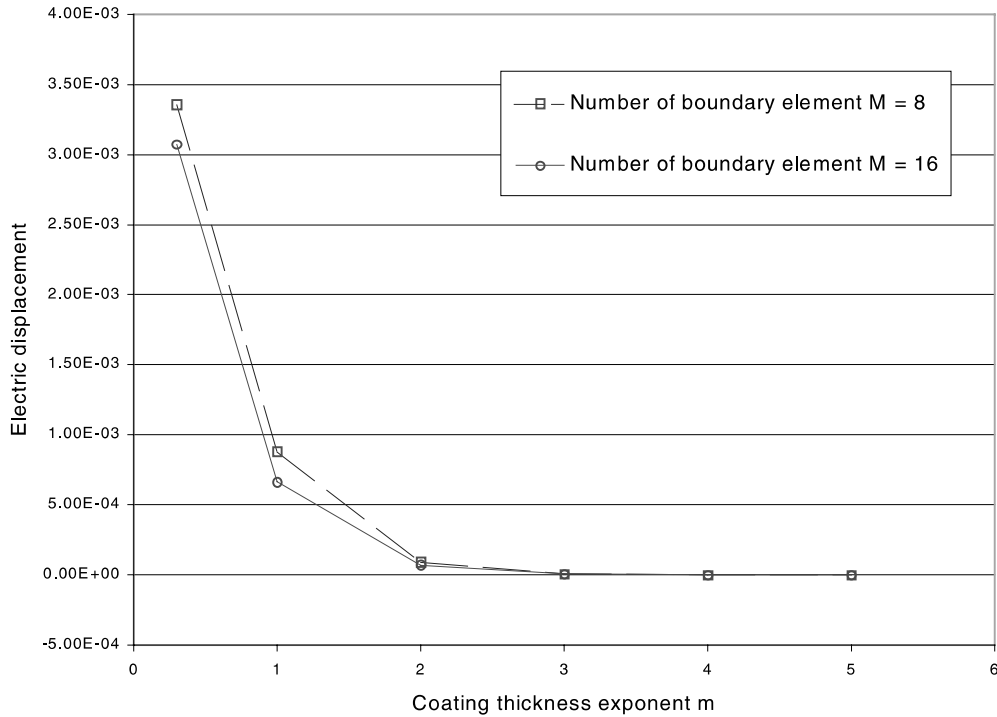


Fig. 9. Magnitude of the electric displacement $D_y (\times p)$ at point B .

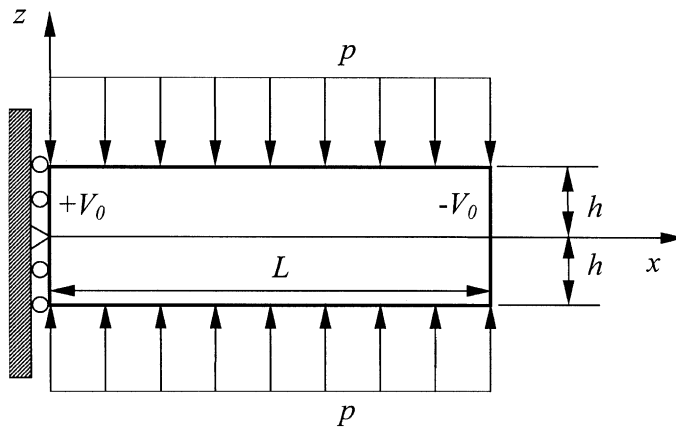


Fig. 10. A PZT-5 strip subjected to pressure load p and voltage V_0 .

easily and may be applied to analyze MEMS problems in which many beam-like piezoelectric structures exist.

All the test problems studied in this section are, of course, relatively simple regarding the geometry and loading conditions. The purpose of these studies is to validate the techniques developed for computing the nearly singular integrals in the piezoelectric BEM. Investigations are underway to apply the developed

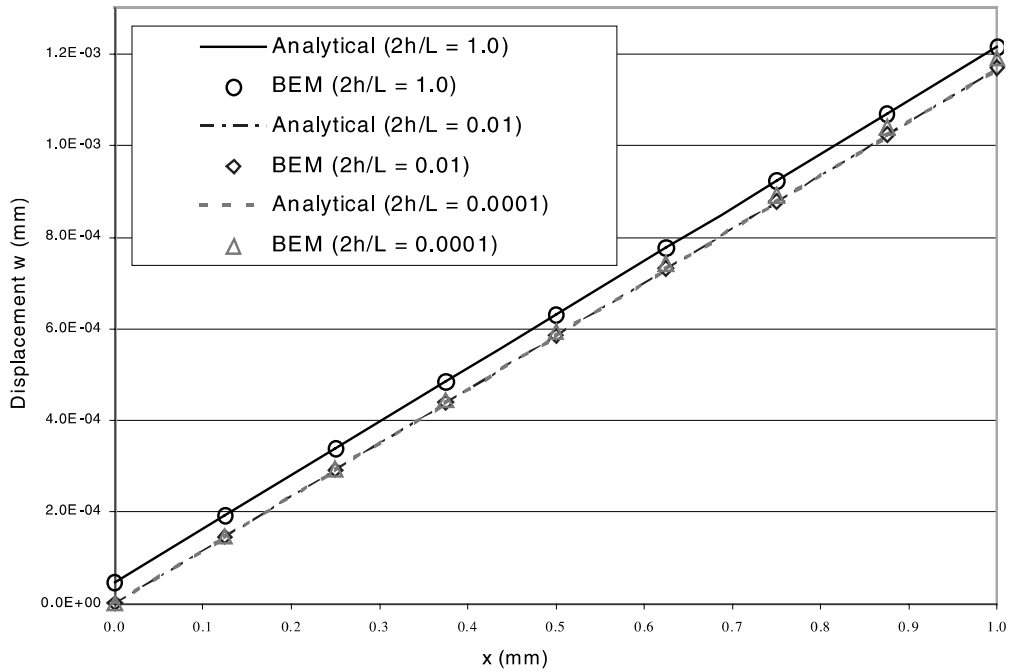


Fig. 11. Displacement w along the bottom edge of the PZT-5 strip for different thicknesses.

piezoelectric BEM to problems of thin and multi-layered piezoelectric films and coatings with more realistic geometry and loading conditions.

5. Conclusion

An advanced 2-D piezoelectric BEM has been developed for the analysis of thin piezoelectric solids. A analytical method has been devised for computing the nearly singular integrals in the piezoelectric BEM for such applications. The numerical results show that the developed piezoelectric BEM is very accurate and efficient for the analysis of thin piezoelectric films and coatings. It is also shown numerically that the piezoelectric BIE does not degenerate when applied to thin piezoelectric solids, as has been proved analytically in Ref. [20]. All these new findings suggest that the BEM can be a very attractive numerical tool for the analysis of piezoelectric films and coatings as employed widely in smart materials, MEMS and other engineering applications.

Acknowledgements

Partial support by the National Science Foundation under the grant CMS 9734949 and by the University of Cincinnati Research Council are gratefully acknowledged. The authors thank Dr. L.Z. Jiang at General Electric for the helpful discussions and for his providing the expressions of the fundamental solution for 2-D piezoelectric materials. The authors also thank the two anonymous reviewers for their helpful comments and suggestions.

Appendix A. The fundamental solution for 2-D piezoelectric solids

For the completeness and reference, we list here the main results of the 2-D piezoelectric fundamental solution which were first derived in Refs. [5–7].

A.1. The U -components in the 2-D piezoelectric fundamental solution

Introduce the following parameters (similar to L_1 – L_6 used in [5–7]):

$$\begin{aligned} g_1 &= \frac{\ln(p_0^2 r_1^2 + r_2^2)}{2}, & g_4 &= \arctan\left(\frac{r_2 + p_1 r_1}{q_1 r_1}\right), \\ g_2 &= \frac{\ln\left[\frac{(p_1 r_1 + r_2)^2 + q_1^2 r_1^2}{2}\right]}{2}, & g_5 &= \arctan\left(\frac{r_2 - p_1 r_1}{q_1 r_1}\right), \\ g_3 &= \frac{\ln\left[\frac{(p_1 r_1 - r_2)^2 + q_1^2 r_1^2}{2}\right]}{2}, & g_6 &= \arctan\left(\frac{r_2}{p_0 r_1}\right); \end{aligned} \quad (\text{A.1})$$

and the parameters [5–7]:

$$\begin{aligned} I_0 &= R_0 g_1 + P_0 (g_2 + g_3) + Q_0 (g_4 - g_5), \\ I_1 &= R_1 g_6 + P_1 (g_4 + g_5) + Q_1 (g_3 - g_2), \\ I_2 &= R_2 g_1 + P_2 (g_2 + g_3) + Q_2 (g_4 - g_5), \\ I_3 &= R_3 g_6 + P_3 (g_4 + g_5) + Q_3 (g_3 - g_2), \\ I_4 &= R_4 g_1 + P_4 (g_2 + g_3) + Q_4 (g_4 - g_5); \end{aligned} \quad (\text{A.2})$$

then the U -components in the 2-D piezoelectric fundamental solution can be expressed as:

$$\begin{aligned} U_{11} &= \frac{1}{2\pi} (\alpha_{11} I_4 + \beta_{11} I_2 + \gamma_{11} I_0), \\ U_{21} &= \frac{1}{2\pi} (\alpha_{12} I_3 + \beta_{12} I_1), \\ U_{31} &= -\frac{1}{2\pi} (\alpha_{13} I_3 + \beta_{13} I_1), \\ U_{12} &= U_{21}, \\ U_{22} &= \frac{1}{2\pi} (\alpha_{22} I_4 + \beta_{22} I_2 + \gamma_{22} I_0), \\ U_{32} &= -\frac{1}{2\pi} (\alpha_{23} I_4 + \beta_{23} I_2 + \gamma_{23} I_0), \\ U_{13} &= \frac{1}{2\pi} (\alpha_{13} I_3 + \beta_{13} I_1), \\ U_{23} &= \frac{1}{2\pi} (\alpha_{23} I_4 + \beta_{23} I_2 + \gamma_{23} I_0), \\ U_{33} &= -\frac{1}{2\pi} (\alpha_{33} I_4 + \beta_{33} I_2 + \gamma_{33} I_0), \end{aligned} \quad (\text{A.3})$$

where α_{ij} , β_{ij} , γ_{ij} , R_i , P_i , Q_i , p_0 , p_1 , and q_1 are parameters related to the material constants, as defined in Refs. [5–7]; and r_1 and r_2 are given in Eq. (17).

A.2. The T -components in the 2-D piezoelectric fundamental solution

The generalized traction kernels T_{ij} are obtained by taking the derivatives of the generalized displacement kernel U_{ij} and applying the relations as specified in Eqs. (3)–(8). First, introduce the following parameters (derivatives of g_1, g_2, \dots, g_6 given in (A.1)):

$$\begin{aligned}
 g_{11} &= \frac{p_0^2 r_1}{p_0^2 r_1^2 + r_2^2}, & g_{41} &= \frac{-q_1 r_2}{(p_1 r_1 + r_2)^2 + q_1^2 r_1^2}, \\
 g_{12} &= \frac{r_2}{p_0^2 r_1^2 + r_2^2}, & g_{42} &= \frac{q_1 r_1}{(p_1 r_1 + r_2)^2 + q_1^2 r_1^2}, \\
 g_{21} &= \frac{(p_1^2 + q_1^2) r_1 + p_1 r_2}{(p_1 r_1 + r_2)^2 + q_1^2 r_1^2}, & g_{51} &= \frac{-q_1 r_2}{(p_1 r_1 - r_2)^2 + q_1^2 r_1^2}, \\
 g_{22} &= \frac{p_1 r_1 + r_2}{(p_1 r_1 + r_2)^2 + q_1^2 r_1^2}, & g_{52} &= \frac{q_1 r_1}{(p_1 r_1 - r_2)^2 + q_1^2 r_1^2}, \\
 g_{31} &= \frac{(p_1^2 + q_1^2) r_1 - p_1 r_2}{(p_1 r_1 - r_2)^2 + q_1^2 r_1^2}, & g_{61} &= \frac{-p_0 r_2}{p_0^2 r_1^2 + r_2^2}, \\
 g_{32} &= \frac{r_2 - p_1 r_1}{(p_1 r_1 - r_2)^2 + q_1^2 r_1^2}, & g_{62} &= \frac{p_0 r_1}{p_0^2 r_1^2 + r_2^2};
 \end{aligned} \tag{A.4}$$

and

$$\begin{aligned}
 I_{01} &= R_0 g_{11} + P_0 (g_{21} + g_{31}) + Q_0 (g_{41} - g_{51}), \\
 I_{11} &= R_1 g_{61} + P_1 (g_{41} + g_{51}) + Q_1 (g_{31} - g_{21}), \\
 I_{21} &= R_2 g_{11} + P_2 (g_{21} + g_{31}) + Q_2 (g_{41} - g_{51}), \\
 I_{31} &= R_3 g_{61} + P_3 (g_{41} + g_{51}) + Q_3 (g_{31} - g_{21}), \\
 I_{41} &= R_4 g_{11} + P_4 (g_{21} + g_{31}) + Q_4 (g_{41} - g_{51}), \\
 I_{02} &= R_0 g_{12} + P_0 (g_{22} + g_{32}) + Q_0 (g_{42} - g_{52}), \\
 I_{12} &= R_1 g_{62} + P_1 (g_{42} + g_{52}) + Q_1 (g_{32} - g_{22}), \\
 I_{22} &= R_2 g_{12} + P_2 (g_{22} + g_{32}) + Q_2 (g_{42} - g_{52}), \\
 I_{32} &= R_3 g_{62} + P_3 (g_{42} + g_{52}) + Q_3 (g_{32} - g_{22}), \\
 I_{42} &= R_4 g_{12} + P_4 (g_{22} + g_{32}) + Q_4 (g_{42} - g_{52});
 \end{aligned} \tag{A.5}$$

and finally

$$\begin{aligned}
 U_{111} &= \frac{1}{2\pi} (\alpha_{11} I_{41} + \beta_{11} I_{21} + \gamma_{11} I_{01}), \\
 U_{211} &= \frac{1}{2\pi} (\alpha_{12} I_{31} + \beta_{12} I_{11}), \\
 U_{311} &= -\frac{1}{2\pi} (\alpha_{13} I_{31} + \beta_{13} I_{11}),
 \end{aligned}$$

$$\begin{aligned}
 U_{121} &= U_{211}, \\
 U_{221} &= \frac{1}{2\pi}(\alpha_{22}I_{41} + \beta_{22}I_{21} + \gamma_{22}I_{01}), \\
 U_{321} &= -\frac{1}{2\pi}(\alpha_{23}I_{41} + \beta_{23}I_{21} + \gamma_{23}I_{01}), \\
 U_{131} &= \frac{1}{2\pi}(\alpha_{13}I_{31} + \beta_{13}I_{11}), \\
 U_{231} &= \frac{1}{2\pi}(\alpha_{23}I_{41} + \beta_{23}I_{21} + \gamma_{23}I_{01}), \\
 U_{331} &= -\frac{1}{2\pi}(\alpha_{33}I_{41} + \beta_{33}I_{21} + \gamma_{33}I_{01}), \\
 U_{112} &= \frac{1}{2\pi}(\alpha_{11}I_{42} + \beta_{11}I_{22} + \gamma_{11}I_{02}), \\
 U_{212} &= \frac{1}{2\pi}(\alpha_{12}I_{32} + \beta_{12}I_{12}), \\
 U_{312} &= -\frac{1}{2\pi}(\alpha_{13}I_{32} + \beta_{13}I_{12}), \\
 U_{122} &= U_{212}, \\
 U_{222} &= \frac{1}{2\pi}(\alpha_{22}I_{42} + \beta_{22}I_{22} + \gamma_{22}I_{02}), \\
 U_{322} &= -\frac{1}{2\pi}(\alpha_{23}I_{42} + \beta_{23}I_{22} + \gamma_{23}I_{02}), \\
 U_{132} &= \frac{1}{2\pi}(\alpha_{13}I_{32} + \beta_{13}I_{12}), \\
 U_{232} &= \frac{1}{2\pi}(\alpha_{23}I_{42} + \beta_{23}I_{22} + \gamma_{23}I_{02}), \\
 U_{332} &= -\frac{1}{2\pi}(\alpha_{33}I_{42} + \beta_{33}I_{22} + \gamma_{33}I_{02});
 \end{aligned} \tag{A.6}$$

then the T -components in the 2-D piezoelectric fundamental solution can be written as

$$\begin{aligned}
 T_{11} &= (c_{11}U_{111} + c_{12}U_{122} + e_{21}U_{132})n_1 + (c_{33}(U_{112} + U_{121}) + e_{13}U_{131})n_2, \\
 T_{21} &= (c_{11}U_{211} + c_{12}U_{222} + e_{21}U_{232})n_1 + (c_{33}(U_{212} + U_{221}) + e_{13}U_{231})n_2, \\
 T_{31} &= (c_{11}U_{311} + c_{12}U_{322} + e_{21}U_{332})n_1 + (c_{33}(U_{312} + U_{321}) + e_{13}U_{331})n_2, \\
 T_{12} &= (c_{12}U_{111} + c_{22}U_{122} + e_{22}U_{132})n_2 + (c_{33}(U_{112} + U_{121}) + e_{13}U_{131})n_1, \\
 T_{22} &= (c_{12}U_{211} + c_{22}U_{222} + e_{22}U_{232})n_2 + (c_{33}(U_{212} + U_{221}) + e_{13}U_{231})n_1, \\
 T_{32} &= (c_{12}U_{311} + c_{22}U_{322} + e_{22}U_{332})n_2 + (c_{33}(U_{312} + U_{321}) + e_{13}U_{331})n_1, \\
 T_{13} &= -(e_{13}(U_{112} + U_{121}) - \varepsilon_{11}U_{131})n_1 - (e_{21}U_{111} + e_{22}U_{122} - \varepsilon_{22}U_{132})n_2, \\
 T_{23} &= -(e_{13}(U_{212} + U_{221}) - \varepsilon_{11}U_{231})n_1 - (e_{21}U_{211} + e_{22}U_{222} - \varepsilon_{22}U_{232})n_2, \\
 T_{33} &= -(e_{13}(U_{312} + U_{321}) - \varepsilon_{11}U_{331})n_1 - (e_{21}U_{311} + e_{22}U_{322} - \varepsilon_{22}U_{332})n_2;
 \end{aligned} \tag{A.7}$$

where the material constants $c_{11}, c_{12}, \dots, \varepsilon_{22}$ are as defined in Refs. [5–7], and n_1 and n_2 are the directional cosines of the normal n .

References

- [1] H.F. Tiersten, *Linear Piezoelectric Plate Vibrations*, Plenum Press, New York, 1969.
- [2] H.S. Tzou, *Piezoelectric Shells: Distributed Sensing and Control of Continua*, Kluwer Academic Publishers, Dordrecht, 1993.
- [3] H.T. Banks, R.C. Smith, Y. Wang, *Smart Material Structures—Modeling, Estimation and Control*, Wiley, Chichester, 1996.
- [4] Y.J. Liu, H. Fan, J.S. Yang, Analysis of the shear stress transferred from a partially electroded piezoelectric actuator to an elastic substrate, *Smart Mater. Struct.* 9 (2000) 248–254.
- [5] J.S. Lee, L.Z. Jiang, Boundary element formulation for electro-elastic interaction in piezoelectric materials, in: C.A. Brebbia, J.J. Rencis (Eds.), *Boundary Elements XV*, Computational Mechanics Publications, Worcester, MA, 1993, pp. 609–620.
- [6] J.S. Lee, L.Z. Jiang, A boundary integral formulation and 2D fundamental solution for piezoelectric media, *Mech. Res. Comm.* 21 (1994) 47–54.
- [7] J.S. Lee, Boundary element method for electroelastic interaction in piezoceramics, *Engrg. Anal. Boundary Elements* 15 (1995) 321–328.
- [8] T. Chen, F.Z. Lin, Boundary integral formulations for three-dimensional anisotropic piezoelectric solids, *Comput. Mech.* 15 (1995) 485–496.
- [9] T. Chen, Green's functions and the non-uniform transformation problem in a piezoelectric medium, *Mech. Res. Comm.* 20 (1993) 271–278.
- [10] T. Chen, F.Z. Lin, Numerical evaluation of derivatives of the anisotropic piezoelectric Green's functions, *Mech. Res. Comm.* 20 (1993) 501–506.
- [11] L.R. Hill, T.N. Farris, Three-dimensional piezoelectric boundary element method, *AIAA J.* 36 (1998) 102–108.
- [12] H. Ding, G. Wang, W. Chen, A boundary integral formulation and 2D fundamental solutions for piezoelectric media, *Comput. Meth. Appl. Mech. Engrg.* 158 (1998) 65–80.
- [13] H. Ding, J. Liang, The fundamental solutions for transversely isotropic piezoelectricity and boundary element method, *Comput. Struct.* 71 (1999) 447–455.
- [14] L.Z. Jiang, Integral representation and Green's functions for 3D time dependent thermo-piezoelectricity, *Int. J. Solids Struct.* 37 (2000) 6155–6171.
- [15] X.-L. Xu, R.K.N.D. Rajapakse, Boundary element analysis of piezoelectric solids with defects, *Composites Part B—Engineering* 29 (1998) 655–669.
- [16] M.H. Zhao, Y.P. Shen, G.N. Liu, Y.J. Liu, Fundamental solutions for infinite transversely isotropic piezoelectric media, in: P. Santini, M. Marchetti, C.A. Brebbia (Eds.), *Computational Methods for Smart Structures and Materials*, WIT Press/Computational Mechanics Publications, Boston, 1998, pp. 45–54.
- [17] M.H. Zhao, Y.P. Shen, G.N. Liu, Y.J. Liu, Dugdale model solutions for a penny-shaped crack in three-dimensional transversely isotropic piezoelectric media by boundary-integral equation method, *Engrg. Anal. Boundary Elements* 23 (1999) 573–576.
- [18] E. Pan, A BEM analysis of fracture mechanics in 2D anisotropic piezoelectric solids, *Engrg. Anal. Boundary Elements* 23 (1999) 67–76.
- [19] Q. Qin, Thermo-electroelastic analysis of cracks in piezoelectric half-space by BEM, *Comput. Mech.* 23 (1999) 353–360.
- [20] Y.J. Liu, H. Fan, On the conventional boundary integral equation formulation for piezoelectric solids with defects or of thin shapes, *Engrg. Anal. Boundary Elements* 25 (2001) 77–91.
- [21] Y.J. Liu, Analysis of shell-like structures by the boundary element method based on 3D elasticity: formulation and verification, *Int. J. Numer. Meth. Engrg.* 41 (1998) 541–558.
- [22] S. Mukherjee, On boundary integral equations for cracked and for thin bodies, *Math. Mech. Solids* 6 (2001) 47–64.
- [23] J.F. Luo, Y.J. Liu, E.J. Berger, Analysis of two-dimensional thin structures (from micro- to nano-scales) using the boundary element method, *Comput. Mech.* 22 (1998) 404–412.
- [24] S.H. Chen, Y.J. Liu, A unified boundary element method for the analysis of sound and shell-like structure interactions. I. Formulation and verification, *J. Acoust. Soc. Am.* 103 (1999) 1247–1254.
- [25] J.F. Luo, Y.J. Liu, E.J. Berger, Interfacial stress analysis for multi-coating systems using an advanced boundary element method, *Comput. Mech.* 24 (2000) 448–455.
- [26] Y.J. Liu, N. Xu, J.F. Luo, Modeling of interphases in fiber-reinforced composites under transverse loading using the boundary element method, *J. Appl. Mech.* 67 (2000) 41–49.
- [27] Y.J. Liu, N. Xu, Modeling of interface cracks in fiber-reinforced composites with the presence of interphases using the boundary element method, *Mech. Mater.* 32 (2000) 769–783.
- [28] X.L. Chen, Y.J. Liu, Multiple-cell modeling of fiber-reinforced composites with the presence of interphases using the boundary element method, *Comput. Mater. Sci.* 21 (2001) 86–94.
- [29] X.L. Chen, Y.J. Liu, Thermal stress analysis of multi-layer thin films and coatings by an advanced boundary element method, *CMES: Comput. Model. Engrg. Sci.* 2 (2001) 337–350.
- [30] Y.J. Liu, T.J. Rudolph, Some identities for fundamental solutions and their applications to weakly singular boundary element formulations, *Engrg. Anal. Boundary Elements* 8 (1991) 301–311.

- [31] Y.J. Liu, On the simple-solution method and non-singular nature of the BIE/BEM—a review and some new results, *Engrg. Anal. Boundary Elements* 24 (2000) 787–793.
- [32] T.A. Cruse, J.D. Richardson, Non-singular Somigliana stress identities in elasticity, *Int. J. Numer. Meth. Engrg.* 39 (1996) 3273–3304.
- [33] J.D. Richardson, T.A. Cruse, Weakly singular stress—BEM for 2D elastostatics, *Int. J. Numer. Meth. Engrg.* 45 (1999) 13–35.
- [34] M. Tanaka, V. Sladek, J. Sladek, Regularization techniques applied to boundary element methods, *Appl. Mech. Rev.* 47 (1994) 457–499.
- [35] V. Sladek, J. Sladek (Eds.), *Singular Integrals in Boundary Element Methods*, Advances in Boundary Element Series, Computational Mechanics Publications, Boston, 1998.
- [36] Y.J. Liu, D.M. Zhang, F.J. Rizzo, Nearly singular and hypersingular integrals in the boundary element method, in: C.A. Brebbia, J.J. Rencis (Eds.), *Boundary Elements XV*, Computational Mechanics Publications, Worcester, MA, 1993, pp. 453–468.
- [37] S. Mukherjee, M.K. Chati, X.L. Shi, Evaluation of nearly singular integrals in boundary element contour and node methods for three-dimensional linear elasticity, *Int. J. Solids Struct.* 37 (2000) 7633–7654.
- [38] R.R. Ohs, N.R. Aluru, Meshless analysis of piezoelectric devices, *Comput. Mech.* 27 (2001) 23–26.